Article:

Carrivick, JL, Smith, MW and Carrivick, DM (2015) Terrestrial laser scanning to deliver high-resolution topography of the upper Tarfala valley, arctic Sweden. GFF, 137 (4). pp. 383-396. ISSN 1103-5897

https://doi.org/10.1080/11035897.2015.1037569 *published in GFF 2015*

Terrestrial laser scanning to deliver high-resolution topography of the upper Tarfala valley, arctic Sweden

Jonathan L. Carrivick[1]*, Mark W. Smith[1], Daniel M. Carrivick[2]

[1]water@leeds and School of Geography, University of Leeds, Woodhouse Lane, Leeds, West Yorkshire, LS2 9JT, UK

[2] 7 Old Farm Road, West Ashton, Trowbridge, Wiltshire, BA14 6FP

*Correspondence to:
Dr. Jonathan Carrivick
Email: j.l.carrivick@leeds.ac.uk
Tel.: 0113 343 3324

Abstract

Alpine valleys are experiencing rapidly changing physical, biological and geochemical processes as glacier masses diminish, snowfall patterns change and consequently as hillslopes and valley-floor landforms and sediments adjust. Measurement and understanding of these processes on a valley, landform and surface scale requires topographic data with sufficient spatial coverage and spatial resolution to resolve sources, fluxes and storages of sediment. Most ideally such topographic data will be of a resolution sufficient to resolve important spatial heterogeneity in land cover, topography and surface texture, for example. This study presents the first high-resolution (1 m grid cell size) and freely-available topography for the upper part of the Tarfala valley, arctic Sweden. The topography was obtained using terrestrial laser scanning (TLS) and a bespoke workflow is presented to most efficiently cover a 9.3 km^2 area. The unprecedented spatial resolution of this topography, which is 15 times greater than that previously available, reveals a suite of alpine landforms. These landforms span multiple glacier forefields, a variety of bedrock surfaces, various hillslopes and types of mass movement, and valley floor glacial, fluvial and periglacial sediments, for example. Primary and second-order derivatives of this elevation data, and vertical transects are given and will assist future classification of landforms and thus assist future targeted field campaigns. Overall, this study presents (i) baseline data from which future re-surveys will enable quantitative analysis of a dynamic landscape, and (ii) An efficient workflow that is readily transferable to any scientific study at any other site. Both of these project outputs will find widespread usage in future alpine studies.

Keywords: terrestrial laser scanner; LiDAR; Storglaciären; arctic; alpine; geomorphology

Background and rationale

Climate change poses a considerable threat to the physical stability, water budget and biodiversity of alpine valleys. Alpine valley hillslopes are destabilising as glacier ice retreats and thins, and as permafrost decays (e.g. Keiler et al., 2010; Stoffel & Huggel, 2012; Keller-Pirklbauer et al., 2012). Continued negative glacier mass-balance will lead to future reductions in glacier runoff (Barnett et al., 2005). Progressively warming air temperatures will lead to less snowfall. Thus ice melt and snow melt will become superseded by groundwater contributions (e.g. Brown et al., 2007a). Changes in both ice melt and snow melt regimes will provoke changes in proglacial river hydrology, hillslope morphology and in valley floor erosion and deposition dynamics (e.g. Carrivick et al., 2013a). Changes in river hydrology; specifically planform, sediment and physico-chemical dynamics, will dramatically alter fluxes of water and sediment (e.g. Malard et al., 2006) and alpine river communities (e.g. Brown et al., 2007b; Brown & Milner, 2012; Jacobsen et al., 2012).

Tarfala valley is typical of many alpine valleys; it is a rapidly changing environment, but it is notable for its exceptional history of glaciological studies (Schytt, 1968; Holmlund & Jansson, 2002) and related geomorphological and bio-geochemical studies. Storglaciären is one of the most intensively studied glaciers in the World (Holmlund, 1996; Holmlund & Jansson, 2002) and the continuous mass-balance record now spans over 70 years. The progress of 20th Century deglaciation in the upper Tarfala valley is well documented with repeated glacier terminus position surveys. Given this high global status of Tarfala in glaciology and in related disciplines, it is perhaps surprising that previous valley-wide topographical measurements and mapping at Tarfala have been at a coarse resolution, and if at a fine-resolution then largely phenomena-specific and published in analogue form (**Table 1**). This has limited the usefulness of these previous topographic measurements for other researchers interested in quantitative land surface analysis, change-detection and process-driven explanation.

The aims of this study are to: (i) present high resolution (sub-metre) topographic survey of the upper Tarfala valley derived using Terrestrial Laser Scanning (TLS), and; (ii) thereby to define a detailed workflow for long-range TLS. The 1 m grid cell resolution digital elevation model of Tarfala valley is freely available for research and teaching use at: http://geo-stage.leeds.ac.uk/research/rbpm/outputs/jcarrivick/ after entering in name, purpose and address details.

Study area

Tarfala is located 120 km west from Kiruna and 25 km north-west of the Sami village Nikkaluokta in arctic Sweden (**Fig. 1A**). The Tarfala valley is a part of the alpine Kebnekaise Mountains. The valley extends in elevation from 700 to 2100 m.asl. and includes Storglaciären, Isfallsglaciären, Kebnepakteglaciären and Sydöstra Kaskasatjåkkaglaciären (**Fig. 1B**). Geologically, the Tarfala valley is part of the late Precambrian Seve belt of the Scandinavian Caledonides. It is dominated by three major tectonic units, notably the Tarfala amphibolite, the Storglaciären gneiss and the Kebne dyke complex (Andréasson & Gee, 1989). Permafrost in the Tarfala catchment is sporadic (Fuchs, 2013). Vegetation in the upper Tarfala valley is patchy and dominated by moss, grass and other high-alpine flora (Fuchs, 2013). Climatically, the mean annual air temperature (1965–2008) at the Tarfala Research Station (1130 m.asl.) is -3.5 ± 0.9 ^{o}C (Grudd & Schneider, 1996, updated with unpublished data of Tarfala Research Station). The mean annual precipitation (since 1989) amounts to 1000 mm a^{-1} (Holmlund & Jansson, 2002).

Survey design

In overview, data from which a near-seamless high resolution (~ 1 m) digital elevation model can be generated requires either: (i) commercial-grade satellite imagery; (ii) an aerial photography campaign with survey-grade digital cameras combined with traditional photogrammetry processing; (iii) an airborne Light Detection and Ranging (LiDAR; ALS) survey; (iv) ground-based Terrestrial Laser Scanning (LiDAR; TLS); or (v) airborne-based or ground-based hand-held photography with and Structure from Motion (SfM) post-processing (Carrivick et al., 2013b). The first three of these options are prohibitively expensive due to the use of an airborne platform. Ground-based SfM was a possibility (e.g. Smith et al., 2014) but would also be very slow in the field (and hence expensive in surveyor time) because of the very large number of viewpoints and photographs and ground control that would be required given the scale of the Tarfala valley. Post-processing of such a large ground-based dataset would require considerable computing power and could be potentially unreliable. We therefore planned a terrestrial laser scanning (TLS) survey, budgeting 8 days fieldwork including two days as contingency for bad weather to cover an area of interest of ~ 8 km^2.

For maximum efficiency in the field, our survey of the Tarfala valley was planned (**Fig. 2**) in a Geographical Information System (GIS) with the aid of: (i) a scanned and georeferenced

1:250,000 regional geomorphological map by Melander (1975); (ii) 1:50,000 vector data of contours, rivers, lakes, roads, glacier outlines from Lantmäteriet (The Swedish Land Survey), mostly from surveys 1980 to 1990; (iii) a scanned and georeferenced topographic map (Holmlund and Schytt, 1987); and (iv) a 15 m grid resolution Digital Elevation Model created by digitising of the Holmlund and Schytt map by Johansson et al. (1999).

Eleven scan positions were sited to: (i) be accessible by foot and at some elevation above the primary surface of interest to give good depth and breadth of coverage, and to minimise occlusion effects in each scan, and; (ii) to most efficiently scan the valley from different angles to avoid data 'shadows' in the final point cloud. This 'most efficient' survey design (**Fig. 1B**) was created with ArcGIS 'viewshed analysis' of scanner positions, coupled with consideration that our scanner; a Riegl VZ-1000 (**Fig. 3A**), has a maximum range of 1400 m. Target-based registration of individual scans was our preferred workflow (**Fig. 2**), and from previous experience we knew that the maximum range for automatic detection of Leica 0.15 m diameter TLS targets (**Fig. 1B**) is 600 m from a scan position, so we specified a 'buffer' at 500 m distance in our GIS (**Fig. 1B**). With a minimum of three targets required for scan registration with an error term, we imposed the condition that at least four targets must be common to more than one scan position (**Fig. 1B**). Finally, since the targets were used not only to merge scans from different scan positions but also to georeference the resultant point cloud, their 3D position in global coordinates was surveyed with dGPS. We therefore conducted an ArcGIS 'skyline' and 'skyplot' analysis (**Fig. 1B**) prior to the survey to check the likelihood of achieving good positional accuracy with a global positioning system (GPS).

Field methods

Long range high resolution terrestrial laser scanning

A Riegl VZ-1000 (**Fig. 3A**) was used to provide high resolution topographic data across the survey area. The VZ-1000 uses a narrow Class 1 infrared laser beam with a manufacturer-stated precision of 0.005 m and accuracy of 0.008 m. The maximum data acquisition rate is 122,000 points per second. However, this rate is limited to surveys of a maximum range of 450 m. In this study the maximum range was set to 1200 m which yielded 42,000 measurements per second. The maximum range of the instrument is 1400 m but the aforementioned 1200 m setting was thought to provide the best compromise between survey time and range. When visibility was reduced, the maximum range was compromised. Target reflectivity also had an effect on survey range; ice and snow had a much smaller maximum survey range (~ 500 m) in this survey than bare ground rock surfaces, for example.

Angular measurement resolution of the VZ-1000 is <0.0005° and minimum horizontal and vertical step-widths are 0.0024°. This equates to ~ 0.0021 m spacing at 500 m range. In this study larger spacings were implemented to decrease survey time; specifically a nominal spatial resolution of 0.2 m at 200 m range was applied. However, in practice the spatial resolution of points depends not only on range but also on relative orientation of a surface owing to the angle of incidence.

Laser beam divergence is a key consideration in designing a long range TLS survey. Beam width at the scanner origin is typically several mm, but the laser beam will diverge with increasing range from the TLS. The manufacturer-stated beam divergence of the VZ-1000 is 0.003 mm per metre of range. Thus, at a range of 500 m the beam width will be approximately 0.015 m. It follows that all surfaces > 0.015 m in diameter were surveyed by the same laser return and the results aggregated in the returning waveform. Where sharp boundaries existed (e.g. built structures) 'mixed pixels' could result whereby a single laser pulse covered both the foreground on the sharp edge and the background some distance away (Lichti et al., 2005). The resulting trail of pixels leading away in a line from the sharp edge towards the background as each return contained a differing proportion of background and foreground can be obvious but since full waveform processing was not available in this survey, results were interpreted (manually) carefully. It must be noted that natural surfaces rarely contain such sharp breaks so this artefact problem was very rare for us in this study. Where such artefacts arise regularly, Hodge et al. (2009a, 2009b) and Smith et al. (2012) outline the use of a series of point filters applied to TLS data to remove any such non-surface points.

Integrated biaxial inclination sensors in the TLS ensured verticality was maintained throughout (accurate to ±0.008°). Following the survey design described above, 11 individual scans were conducted to ensure that each surface was scanned from a minimum range of 500 m. At each survey station an overview scan was conducted to orientate the operator in the scanner's local co-ordinate system (< 1 minute duration). Using this overview scan and a ruggardised field laptop, a window was drawn to limit the full scan to only the area of interest and to avoid, where possible, using valuable survey time to create unnecessarily high resolution point clouds of nearby surfaces (i.e. cliff walls). Each full scan was of ~ 45 minutes duration. Target acquisition (described below) added another 20 to 30 minutes at the scan position (**Fig. 3A**). Thus, overall, activity at each scan position (**Fig. 2**) required ~ 1hr 15 minutes of surveying, plus the time taken to relocate the TLS and targets between scans. The VZ-1000 is reasonably portable, weighing 9.8 kg plus battery weight and was transported between stations in a Peli-case fitted with rucksack straps.

Following inspection of the resulting point cloud, a further two scans were added to the survey to provide a better perspective of glacier forefields and to fill small data gaps in the topographic model that were caused by shadowing from small scale topography not represented in the previously available DEM. All scans were merged to produce a final point cloud of > 1bn survey observations over the target survey area of ~ 9 km^2.

Registration of scans

Whilst the VZ-1000 contains an integrated GPS receiver, it is single phase and thus with relatively limited accuracy so this was not used for 'stand-alone' registration. Instead, a target-based registration was performed to merge the individual scans into a single point cloud of the entire valley. Target-based registration was preferred to methods reliant upon automated and iterative matching of separate point clouds (cloud-based registration) owing primarily to the high accuracy desirable. Secondarily, target-based registration permitted rapid registration of scans in the field yielding instant results (e.g. **Fig. 4**) and facilitating manual checks for blunders.

Six Leica 0.15 m diameter targets were distributed around each scan position. The targets were elevated above the local surface on mini-tripods to increase their visibility at longer ranges and could be swivelled to face any orientation. Target position geometry aimed to provide the greatest possible coverage of horizontal angles to provide robust registration. The arbitrary co-ordinates of the first (southernmost) scan were used throughout the survey. All targets were precisely scanned from the first scan position; the VZ-1000 was calibrated to recognise and fine-scan each target to obtain an accurate fix on the 3D location of the target centroid. Note, these 'fine' or 'target' scans did not form part of the final point cloud. For fine scanning, a target had to be located < 500 m from the TLS as incorporated into the survey design.

As the survey traversed northwards up the valley a minimum of 4 established targets (i.e. tied into the station 1 co-ordinate system) were required to accurately locate and orientate each new point cloud in the arbitrary co-ordinate system using a rigid body similarity transformation. Registration errors of each survey were thus obtained (**Table 2**). Once each scan was complete redundant targets were 'leap-frogged' up the valley and resurveyed to be 'tied-in' for subsequent scans. The survey traversed up the valley in this manner for 4 field days.

As described above, owing to good weather during the survey period, a further two scans were conducted opportunistically in areas of particular interest. Unlike the majority of scans, these were manually registered into the arbitrary co-ordinate system of the valley scan using available 'pick-points' in both point clouds. As before, a minimum of four common points was used to register the scans. The completeness of the valley scan meant that identifying such common points was relatively straightforward, with distinct features (buildings, telegraph poles, tents poles) favoured. As expected, registration errors of these extra two scans were greater than those from target-based registration (**Table 2**) but are acceptable given the overall scale and purpose of the valley survey.

Accurate positioning of targets

Targets were precisely located in the field using a Leica GPS500, which is a differential dual phase receiver system, with a static 'base station' recording at 1 s intervals. Our points of interest; the targets, were positioned with a 'rover' in static mode (**Fig. 3B**), whereby 180 to 300 readings were averaged per point; the number of points being subjectively determined by the user by assessing number and geometry of satellites.

Post-Processing methods

TLS data

Each point cloud was individually edited to remove artefacts in the scans. These artefacts included Leica targets on tripods, passing tourists, reindeer and the surveyors themselves. Near water surfaces (e.g. running streams and the lake at the head of the valley) were removed. Spectral reflectances arising from the presence of water were identified using point reflectance data and were also removed. Any other clearly erroneous points were removed from each point cloud. This cleaning process took around 1 hour per scan and took place prior to georeferencing.

dGPS data

All rover dGPS positions were post-processed relative to our base station and achieved at least 0.005 m 3D accuracy. Our base station position was positioned via post-processing of 8 hours static data per day (for 5 days) relative to a continuous 'active' dGPS station at Kiruna; a 120 km baseline, and achieved 0.0005 m 3D accuracy. All dGPS surveys were conducted in WGS84 global system latitude and longitude decimal seconds, but converted to coordinates WGS84 UTM zone 34N for assimilation with other datasets and because it is conveniently metric.

Georeferencing

Once the point cloud was registered into a single co-ordinate system, the entire cloud was then georeferenced into a 'real-world' co-ordinate system using a rigid-body transformation (Granshaw, 1980). This workflow was preferable such that the survey itself is merged was seamlessly as possible and errors arising from dGPS georeferencing did not compromise the internal integrity of the point cloud. The final georeferencing error using 27 corresponding tiepoints distributed over the entire valley was 0.27 m.

Data Decimation

Point cloud data were decimated to create a terrain dataset that required less data storage. The open-source topographic point cloud analysis toolkit (ToPCAT) was used to unify point densities and create a Digital Elevation Model (DEM) from the data. For a full description of this intelligent decimation method, see Brasington et al. (2012). ToPCAT returned a large number of sub-grid statistics on a defined grid determined by the defined DEM resolution. Whilst this data is still being analysed, for example with respect to topographic roughness (Smith, 2014), the mean elevation in each grid cell was selected as the appropriate value for DEM construction in this study. While the complete point cloud was dense enough to support a much higher resolution DEM (<0.1 m in places), a DEM resolution of 1 m was selected to provide a manageable and useful valley-wide data set. Overall, the '3D points' per square metre can be represented spatially (**Fig. 5A**) and in frequency (**Fig. 5B**). The highest density of points are close to scan positions (**Fig. 5A**) and **Figure 5B** shows that ~ 85 % of all the 1 m^2 grid cells have > 10 associated elevation points.

Results

The resultant DEM occupied 0.87 Gb in text file format and 1.6 Gb memory in ArcGIS shapefile format and covers a valley length of ~ 5 km, an area of 9.3 km^2 and ranged in elevation from 983 to 1863 m.asl. When gridded at 1 m grid cell size using an inverse distance weighting (IDW) interpolation with a 2 m fixed search radius, the resultant digital elevation model can be represented as a near-continuous surface (**Fig. 6A**) or contour lines (**Fig. 6B**). Gaps in the surface coverage are due to either (i) no laser returns off water surfaces, such as lakes, rivers, streams, snow and wet ice, or (ii) obstruction of the laser due to an obstacle creating 'shadowing'. Primary topographic derivatives including slope (**Fig. 6D**) and aspect (**Fig. 6C**) and secondary topographic derivatives including curvature (**Fig. 6E**) will be useful for quantitative analysis, whereas hillshaded terrain (**Fig. 6F, Fig. 7**) is useful for visualisation.

The 1 m grid cell resolution digital elevation model of Tarfala valley is freely available for research and teaching use at: http://geo-stage.leeds.ac.uk/research/rbpm/outputs/jcarrivick/ after entering in name, purpose and address details.

The complete hillshaded terrain model, as presented in **Figure 7**, illustrates the complexity of the topography of the upper Tarfala valley in unprecedented detail. There will almost certainly be a lot of analysis of this high-resolution topography in subsequent research efforts, but for now we draw attention to the pronounced asymmetry that the upper Tarfala valley has in its topography. Eastern (west-facing) hillslopes are relatively uniform in slope gradient and curvature, relatively uniform in aspect and relatively uniform in micro-topography with incised gullies on steeper upper slopes (in both bedrock and in scree) and low-gradient subdued-relief ground occupying most of the valley floor. In contrast, the western (east-facing) side of upper Tarfala valley is dominated by steep bedrock buttresses from which extensive scree aprons extend, and steep-sided arcuate ridges of moraine.

Many topographic details that would be difficult to observe or measure in the field become apparent in the DEM (**Fig. 7**). For example, on eastern valley hillslopes it is intriguing to see that gullies are restricted to steep slopes and do not have any topographic signature of extending westwards across the valley floor, perhaps suggesting considerable subsurface flow through the porous blockfields. On western slopes it is interesting to note that the easternmost arc of Storglaciären moraine crosses over the primary drainage line of Tarfala valley, implying that when the glacier was at this extended position it would have formed a dam to meltwater sourced from higher up-valley. On hillslopes encircling Tarfalasjon, the axes of gullies changes direction, which permits interpretation of the geological strata and hence faulting in this area. In front of Isfallsglaciären the orientation of flutes reflects former ice flow directions. Minor ridges with SW-NE alignment situated immediately east of Tarfalastugan (Swedish Tourist Federation hut) could be moraines from an advanced Isfallsglaciären. Minor ridges with N-S alignment half way up the eastern hillside could represent moraines and a former advanced and 'coalesced' glacier system. These examples are not with proven interpretations; they are given to illustrate the potential for hypothesis-driven research on the basis of this unprecedented detail of topographic information.

Digital elevation models permit quick measurements of elevation along selected transects and these further aid baseline descriptions of topography, interpretation of landforms, inference of earth surface processes and suggestions of landscape chronology or evolution. By way of example, we present profiles of elevation with distance from the August 2014 terminii of Storglaciären, Isfallsglaciären and Kebnepakteglaciären (**Fig. 8A**). Storglaciären terminus is convex, Isfallsglaciären is linear and Kebnepakteglaciären terminus is convex for the first 100 m and then concave (**Fig. 8A**). Profiles of mass movement deposits on the hillslopes bounding the north of Tarfalajaure are all concave thereby suggesting an abundant supply of sediment, but profile 4 has a convex toe possibly suggesting erosion of that toe slope or a disconnected or transport-limited mass movement system (**Fig. 8B**). The mean gradient of these 9 profiles varies from 0.47 to 0.11; the former representing a likely unstable over-steepened fall deposit, and the latter representing a deposit from a far more fluid flow mass movement (**Fig. 8B**). On a finer scale, a transect across the Isfallsglaciären flutes demonstrates that these are typically 0.5 to 2 m high and whilst the flutes are frequently multi-crested; i.e. with superimposed minor flutes, the inter-flute troughs are narrow and v-shaped (**Fig. 8C**). A transect across the proglacial forefield at Storglaciären (**Fig. 8D**) indicates the discrepancy in elevation of the bounding lateral moraines at this point (they are more similar in elevation more westwards), perhaps indicating either an asymmetric palaeo-glacier terminus or significant melt-out and down-wasting of the moraines as they were/are probably ice-cored (c.f. Ackert, 1984). A transect across the surface of the Storglaciären terminus illustrates asymmetry in micro-topography or surface roughness; the northern side being far smoother than the southern (**Fig. 8E**).

The digital elevation model presented herein is 15 times higher spatial resolution that the previously available DEM of Johansson et al. (1999). A cell by cell comparison of our 1 m resolution model with that 15 m resolution model revealed elevation differences typically of up to 30 m (**Fig. 9**), mainly on the lower elevation valley floor. Some of the elevation differences were expected due to the time elapsed between the different surveys, as explained by thinning of the glacier termini, for example. Some elevation differences were expected due to the differing DEM resolutions. However, the magnitude of the elevation differences was surprising and we made some investigation to see if there were any relationships between the raw and absolute magnitude of elevation differences with slope gradient (**Fig. 10**). We did not find any statistically significant relationships and the elevation differences are not normally distributed, so are not random. Therefore we attribute the elevation differences to be indicative of error in the 15 m DEM, which originally stems from the photogrammetry used to construct the Holmlund and Schytt (1987) map. Specifically, firstly there was likely lack of ground control points in higher-gradient terrain, and secondly photogrammetric DEM error tends to be greatest in steeper and more rugged areas due to the issues of topographic shading and the image-matching algorithms inherently applied (Hopkinson et al. 2009).

Discussion

The 1 m grid resolution DEM will permit spatially extensive yet high resolution observation (**Figs. 6, 7**) and measurement (**e.g. Fig. 8**). For structural geology exposed in the landscape this might include length, azimuth and planar aspect, for example. For geomorphology a range of valley, landform and micro-scale features can be observed (**Fig. 11**) and could be automatically delineated and measured via break of slope and surface texture analyses. Indeed it is quite likely that persons both unfamiliar and familiar with the upper Tarfala valley will view the hillshaded terrain model (**Fig. 7**) and identify interesting, perhaps subtle, features thereby prompting future field investigation. For example, in the results section we have highlighted subtle ridges near Tarfala Turiststation, subtle ridges halfway up the eastern hillslopes and possibilities of subsurface drainage through the eastern valley floor. We have highlighted the obvious east-west asymmetry in the valley curvature and hillslope geomorphology. Our elevation data highlights the contrasts in the glacier termini and also the contrasts in the associated moraines and proglacial forefield topography.

The unprecedented spatial resolution and coverage of topographic survey in upper Tarfala valley as presented here will act as baseline data for repeat surveys, which may be more localised, to detect changes. Glacier terminus retreat and thinning and hence volume change is an obvious example. However, perhaps more could be made of the inter-subcatchment differences between the glaciers and the proglacial glacier forefields, despite having the same prevailing climate and underlying geology. Inter-catchment differences in mass balance response of glaciers to climate and hence inter-catchment differences in proglacial glacier forefields have been highlighted in New Zealand by Carrivick & Chase (2011) and Carrivick & Rushmer (2009), respectively.

Furthermore, given that valley-wide sediment sources, sinks and fluxes are simply unquantified there is plenty of potential for this DEM to be used as a baseline from which to detect hillslope and valley floor elevation changes, volume changes and to calculate rates of change in terms of geomorphological activity. Recognition of geomorphological activity in Tarfala includes field observations and measurements on avalanche boulder tongues (Rapp, 1959), talus/scree movement (Rapp & Strömquist, 1976), ice-cored moraine degradation (Ackert, 1984) and permafrost soil creep (Jahn, 1991). Cewe & Norrbin (1965) and Norrbin (1973), and Schneider & Bronge (1996) examined water levels, suspended sediment and sedimentation in a few discrete reaches of a few streams. Etienne et al. (2003) identified sediment-landform assemblages in Tarfala, but only for the proglacial Storglaciären forefield. Thus previous geomorphological studies in the Tarfala valley have been phenomena-specific and spatially-restricted. Nonetheless they permit anticipation that geomorphological activity in the Tarfala catchment, as detected from future comparison of repeated surveys and DEMs of difference (DoDs), will be diverse; including both continuous and episodic events and both laterally extensive (e.g. periglacial, fluvial) and spatially restricted (e.g. mass movement falls and slumps) processes. Future studies utilising the DEM of this study as a baseline and repeating the survey style, as recommended for quantitatively characterising sediment fluxes by Orwin et al. (2010), will thus be able to identify linkages (c.f. Bertoldi et al., 2009) and hence process-based coupling between different landscape components (c.f. Caine, 1974); i.e. sediment budgets (c.f. Dietrich & Dunne, 1978; Fuller et al., 2003).

The digital elevation model presented herein has near-complete coverage of the Tarfala valley, is high-resolution and is freely available digitally. It will inevitably enable developing process-based understanding via numerical modelling. It is likely to be used for high-resolution surface energy balance modelling, hydrological routing and hydraulic and water quality modelling (e.g. Smith et al., 2011; Carrivick et al., 2012), serving interests and perhaps rapidly developing projects at Tarfala in glaciology, geomorphology, ecology and biogeochemistry.

This study included robust planning using GIS-based analyses to determine the optimal number, position and geometry of scan positions and target positions given constraints imposed by human access, laser scanner hardware capability and dGPS usage for global georeferencing. In just 4 days field time this study produced a very large topographic survey (> 1 billion points over a 9.6 km^2 area) and is perhaps the most areally extensive in the literature; compared to ~ 0.006 km^2 by Milan et al. (2007); 0.3 km^2 by Brasington et al. (2012); 2 km^2 by Williams et al. (2014). Therefore whilst these other studies had higher spatial resolution (point density) and often included repeat surveys, the workflow of this study (**Fig. 2**), which goes beyond the field and processing protocol presented by Heritage & Hetherington (2007), will be of considerable interest to other terrestrial laser scanner users for maximising project efficiency.

Conclusion

The long and distinguished history of research undertaken in the Tarfala valley and in particular on Storglaciären is a resource of global significance. To date, topographic datasets of the Tarfala valley have either been of coarse resolution or of spatially-limited coverage. In this study we made a metre-scale topographic model of the entire Tarfala valley and this is now freely available. It is anticipated that the availability of such high-quality topographic data will stimulate further research at this important location encouraging researchers and students alike to conduct a thorough interrogation of the topography and geomorphology resolved in this model. Moreover, it will serve as baseline data for future re-surveys and thus for quantitative analysis of the dynamic landscape of Tarfala valley. The efficient workflow as presented in this study is readily transferable to any scientific study at any other site. More widely, the DEM will be an important dataset for visualisation (e.g. **Fig. 11**), which will be useful for pre-field work planning, teaching, and ‘popular science’ and ‘outreach’ activities.

Acknowledgements

The research leading to these results has received funding from the European Union Seventh Framework Programme [FP7/2007-2013] under grant agreement n° 262693 [INTERACT]. We thank Kallax Flyg for their excellent logistics assistance. We thank Gunhild Rosqvist and

Torbjörn Karlin and all the summer 2014 Tarfala staff for their help and interest in this project. Two reviewers and the Editor are thanked for their supportive comments.

References

Ackert Jr, R. P.,1984: Ice-cored lateral moraines in Tarfala valley, Swedish Lapland. *Geografiska Annaler. Series A. Physical Geography*, 79-88.

Andréasson, P. G., & Gee, D. G..1989: Bedrock geology and morphology of the Tarfala area, Kebnekaise Mts., Swedish Caledonides. *Geografiska Annaler. Series A. Physical Geography*, 235-239.

Barnett, T. P., Adam, J. C., & Lettenmaier, D. P., 2005: Potential impacts of a warming climate on water availability in snow-dominated regions. Nature, 438(7066), 303-309.

Bertoldi, W., Gurnell, A., Surian, N., Tockner, K., Zanoni, L., Ziliani, L., & Zolezzi, G.,2009: Understanding reference processes: linkages between river flows, sediment dynamics and vegetated landforms along the Tagliamento River, Italy. *River Research and Applications*, *25*(5), 501-516.

Brasington, J., Vericat, D., & Rychkov, I., 2012: Modeling river bed morphology, roughness, and surface sedimentology using high resolution terrestrial laser scanning. Water Resources Research, 48(11).

Brown, L. E., & Milner, A. M., 2012: Rapid loss of glacial ice reveals stream community assembly processes. Global Change Biology, 18(7), 2195-2204.

Brown, Lee E., Alexander M. Milner, and David M. Hannah, 2007a: Groundwater influence on alpine stream ecosystems. Freshwater Biology 52.5 878-890.

Brown, L. E., Hannah, D. M., & Milner, A. M., 2007b: Vulnerability of alpine stream biodiversity to shrinking glaciers and snowpacks. *Global Change Biology*, *13*(5), 958-966.

Carrivick, J. L., & Rushmer, E. L., 2009: Inter-and intra-catchment variations in proglacial geomorphology: an example from Franz Josef Glacier and Fox Glacier, New Zealand. Arctic, Antarctic, and Alpine Research, 41(1), 18-36.

Carrivick, J. L., & Chase, S. E., 2011:Spatial and temporal variability of annual glacier equilibrium line altitudes in the Southern Alps, New Zealand. *New Zealand Journal of Geology and Geophysics*, *54*(4), 415-429.

Carrivick, J. L., Brown, L. E., Hannah, D. M., & Turner, A. G., 2012: Numerical modelling of spatio-temporal thermal heterogeneity in a complex river system. *Journal of Hydrology*, *414*, 491-502.

Carrivick, J. L., Geilhausen, M., Warburton, J., Dickson, N. E., Carver, S. J., Evans, A. J., & Brown, L. E., 2013a: Contemporary geomorphological activity throughout the proglacial area of an alpine catchment. *Geomorphology*, *188*, 83-95.

Carrivick, J. L., Smith, M. W., Quincey, D. J., & Carver, S. J., 2013b: Developments in budget remote sensing for the geosciences. *Geology Today*, *29*(4), 138-143.

Caine, N., 1974: The geomorphic processes of the alpine environment. In: Ives, J.D., Barry, R.G. (Eds.), Arctic and Alpine Environments. Methuen, London, pp. 721– 748.

Cewe, T and Norrbin, J., 1965: Tarfalajaikka; Ladtjojaikka och Ladtjojaure. Vattenföring, slamtransport och sedimentation. Ymer 1-2: 85-111.

Dietrich, W.E., Dunne, T., 1978: Sediment budget for a small catchment in mountainous terrain. Zeitschrift für Geomorphologie. Supplementband 29, 191– 206.

Etienne, J. L., Glasser, N. F., & Hambrey, M. J. , 2003: Proglacial sediment-landform associations of a polythermal glacier: Storglaciären, northern Sweden. *Geografiska Annaler: Series A, Physical Geography*, *85*(2), 149-164.

Fuller, I.C., Large, A.R.G., Charlton, M.E., Heritage, G.L., Milan, D.J., 2003: Reach-scale sediment transfers: an evaluation of two morphological budgeting approaches. *Earth Surface Processes and Landforms* 28, 889–903.

Fuchs, M., 2013: Soil Organic Carbon Inventory and Permafrost Mapping in Tarfala Valley, Northern Sweden: A first estimation of the belowground soil organic carbon storage in a sub-arctic high alpine permafrost environment. Stockholm University, Masters thesis, 109pp.

Granshaw, S.I., 1980: Bundle adjustment methods in engineering photogrammetry. The Photogrammetric Record 10: 181–207.

Grudd, H., & Schneider, T., 1996: Air temperature at Tarfala research station 1946-1995. Geografiska Annaler. Series A. Physical Geography, 115-120.

Heritage, G., & Hetherington, D., 2007:Towards a protocol for laser scanning in fluvial geomorphology. Earth Surface Processes and Landforms, 32(1), 66-74.

Hodge, R., Brasington, J., Richards K., 2009a: In situ characterisation ofgrain-scale fluvial morphology using terrestrial laser scanning. Earth Surface Processes and Landforms 34: 954–968.

Hodge, R., Brasington, J., Richards, K., 2009b: Analysing laser-scanned digital terrain models of gravel bed surfaces: linking morphology to sediment transport processes and hydraulics. Sedimentology 56: 2024–2044.

Holmlund, P., 1996: Maps of Storglaciären and their use in glacier monitoring studies. *Geografiska Annaler. Series A. Physical Geography*, 193-196.

Holmlund, P., & Jansson, P., 2002: Glaciological research at Tarfala research station. Stockholms Universitet.48 pp.

Holmlund, P., & Schytt, V., 1987: Högfjällskartan: Kebnekaise. 1:20,000 sheet map. Lantmäteriert, Stockholm. ISBN 91-588-4264-0.

Hopkinson, C., M. Hayashi & D. Peddle, 2009:Comparing alpine watershed attributes from LiDAR, Photogrammetric, and Contour-based Digital Elevation Models. Hydrological Processes, 23(3), 451-463.

Jacobsen, D., Milner, A. M., Brown, L. E., & Dangles, O., 2012: Biodiversity under threat in glacier-fed river systems. Nature Climate Change, 2(5), 361-364.

Jahn, A., 1991: Slow soil movement in Tarfala valley, Kebnekaise mountains, Swedish Lapland. *Geografiska Annaler. Series A. Physical Geography*, 93-107.

Johansson, M., Ekroth, J., & Johansson, M., 1999: Digital elevation model covering the Tarfala valley and its surroundings. Tarfala Forskningsrappor, 111. 38-41.

Keiler, M., Knight, J., & Harrison, S., 2010: Climate change and geomorphological hazards in the eastern European Alps. Philosophical Transactions of the Royal Society A: Mathematical, Physical and Engineering Sciences, 368(1919), 2461-2479.

Kellerer-Pirklbauer, A., Lieb, G. K., Avian, M., & Carrivick, J., 2012: Climate change and rock fall events in high mountain areas: Numerous and extensive rock falls in 2007 at Mittlerer Burgstall, Central Austria. Geografiska Annaler: Series A, Physical Geography, 94(1), 59-78.

Koblet, T., Gärtner-Roer, I., Zemp, M., Jansson, P., Thee, P., Haeberli, W., & Holmlund, P., 2010: Reanalysis of multi-temporal aerial images of Storglaciären, Sweden (1959–99)–Part 1: Determination of length, area, and volume changes. The Cryosphere, 4(3), 333-343.

Lichti, D.D., Gordon, S.J, Tipdecho, T., 2005: Error models and propagation in directly georeferenced terrestrial laser scanner networks. Journal of Surveying Engineering 131: 135–142.

Malard, F., Uehlinger, U., Zah, R., & Tockner, K., 2006: Flood-pulse and riverscape dynamics in a braided glacial river. Ecology, 87(3), 704-716.

Melander, O., 1975: Geomorfolgiska kartbladet 29: Kebnekaise. Statens Naturvardsverk PM 540. 78pp.

Milan, D. J., Heritage, G. L., & Hetherington, D., 2007: Application of a 3D laser scanner in the assessment of erosion and deposition volumes and channel change in a proglacial river. *Earth surface processes and landforms*, *32*(11), 1657-1674.

Norrbin, J., 1973: Vattenföring och slamtransport i Tarfala och Ladtjojakka 1960-1967. Stockholm University, Department of Physical Geography, 99 p.

Orwin, J. F., Lamoureux, S. F., Warburton, J., & Beylich, A., 2010: A framework for characterizing fluvial sediment fluxes from source to sink in cold environments. *Geografiska Annaler: Series A, Physical Geography*, *92*(2), 155-176.

Pomeroy, J. A., 2013: The sedimentary and geomorphic signature of subglacial processes in the Tarfala Valley, northern Sweden, and the links between subglacial soft-bed deformation, glacier flow dynamics, and landform generation (Doctoral dissertation, Loughborough University).

Rapp, A., 1959: Avalanche boulder tongues in Lappland. *Geografiska Annaler*, *41*(1), 34-48.

Rapp, A., & Strömquist, L., 1976: Slope erosion due to extreme rainfall in the Scandinavian mountains. *Geografiska Annaler. Series A. Physical Geography*, 193-200.

Schneider, T., & Bronge, C. (1996). Suspended sediment transport in the Storglaciären drainage basin. *Geografiska Annaler. Series A. Physical Geography*, 155-161.

Schytt, V., 1968: Notes on glaciological activities in Kebnekaise, Sweden during 1966 and 1967. *Geografiska Annaler. Series A, Physical Geography*, *50*(2), 111-120.

Smith, M.W., 2014: Roughness in the Earth Sciences. Earth Science Reviews 136, 202–225.

Smith, M.W., Cox, N.J. and Bracken, L.J., 2011: Terrestrial laser scanning soil surfaces: a field methodology to examine surface roughness and overland flow hydraulics. *Hydrological Processes* 25, 842−860.

Smith, M.W., Vericat, D., and Gibbins, C., 2012: Through-water terrestrial laser scanning of gravel beds at the patch scale. Earth Surface Processes and Landforms 37, 411-421.

Smith, M.W., Carrivick, J.L., Hooke, J., Kirkby, M.J., 2014: Reconstructing Flash Flood Magnitudes Using 'Structure-from-Motion': a rapid assessment tool. *Journal of Hydrology* 519, 1914–1927.

Stoffel, M., & Huggel, C., 2012: Effects of climate change on mass movements in mountain environments. Progress in Physical Geography, 36(3), 421-439.

Williams, R. D., Brasington, J., Vericat, D., & Hicks, D. M., 2014: Hyperscale terrain modelling of braided rivers: fusing mobile terrestrial laser scanning and optical bathymetric mapping. Earth Surface Processes and Landforms, 39(2), 167-183.

High-resolution topography of the upper Tarfala valley

Jonathan L. Carrivick, Mark W. Smith, Daniel M. Carrivick

Data	Type	Source and comment
National/regional contours	20 m interval, digital vector	Is same as 1:50,000 hard copy maps by Lantmäteriert.
Local 1:20,000 map	10 m contour interval, analogue	Holmlund and Schytt (1987).
Local DEM	15 m grid, digital raster	Johansson et al. (1999) who digitised hard copy of Holmlund and Schytt (1987).
Kebnekaise massif geology	Analogue map	Andréasson and Gee (1989).
Regional geomorphology	Analogue map	Melander (1975).
Local geomorphology	Analogue map(s)	Patch to sub-catchment scale mapping and detailed analysis of avalanche boulder tongues (Rapp, 1959), talus/scree movement (Rapp and Strömquist, 1976), ice-cored moraine degradation (Ackert, 1984) and permafrost soil creep (Jahn, 1991). These studies were phenomena-specific. More recently sediment-landform associations considered by Etienne et al. (2003), Pomeroy (2013), for example.
Storglaciaren historical surfaces	Digital elevation model(s)	Koblet et al. (2010).

Table 1. *Summary of pre-existing published topographic information for Tarfala*

High-resolution topography of the upper Tarfala valley

Jonathan L. Carrivick, Mark W. Smith, Daniel M. Carrivick

Scan Station	Registration Type	Number of Targets / Common Points	Standard deviation (m) (3D error)
1	Targets	-	-
2	Targets	4	0.0079
3	Targets	5	0.0383
4	Targets	6	0.0479
5	Targets	5	0.0328
6	Targets	5	0.0157
7	Targets	5	0.0328
8	Targets	5	0.0266
9	Targets	5	0.0152
10	Targets	5	0.0051
11	Targets	5	0.0090
12	Pick-points	4	0.1472
13	Pick-points	4	0.0957

Table 2. *Scan registration errors*

High-resolution topography of the upper Tarfala valley

Jonathan L. Carrivick, Mark W. Smith, Daniel M. Carrivick

***Figure 1**. Study area location (A) and overview of study area topography and survey design (B). Survey design includes eleven scan positions and thirty target positions, where the target positioning was aided by creation of 500m buffers from scanner and with analysis of skyplot, the latter as represented by circular graphs. Note only one skyline for target 21 is depicted here for clarity. Contours, lakes, rivers and glacier outlines are from Landmateriert (1:50,000) mapping. Black triangles are local ('Tarfala coordinate') reference points as used in many historical surveys. Graticule coordinates in (B) is WGS84 UTM zone 34N.*

High-resolution topography of the upper Tarfala valley

Jonathan L. Carrivick, Mark W. Smith, Daniel M. Carrivick

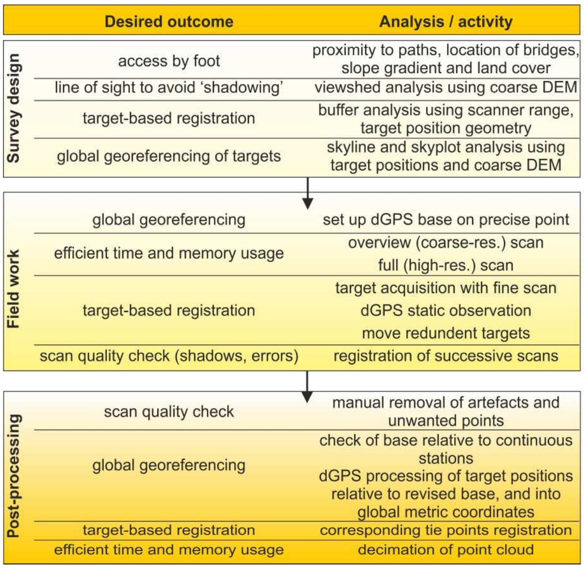

Figure 2. *Summary of workflow presented for the survey design, field work and post-processing phases of this study*

High-resolution topography of the upper Tarfala valley

Jonathan L. Carrivick, Mark W. Smith, Daniel M. Carrivick

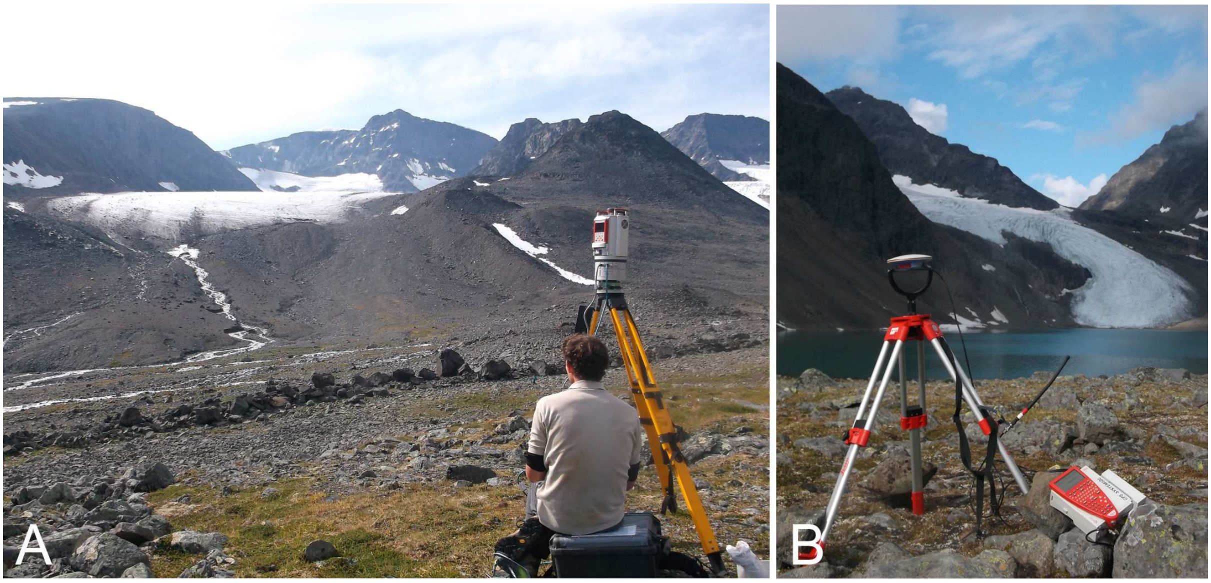

Figure 3. *Illustration of field methods: (A) a terrestrial laser scanner to acquire a 3D point cloud with points up to 1200 m from the scan position at a mean spacing of 0.2 m at 200 m range, and; (B) tripod-mounted targets (x6) and a Leica dGPS used for precise georeferencing of targets and hence of the point clouds.*

High-resolution topography of the upper Tarfala valley

Jonathan L. Carrivick, Mark W. Smith, Daniel M. Carrivick

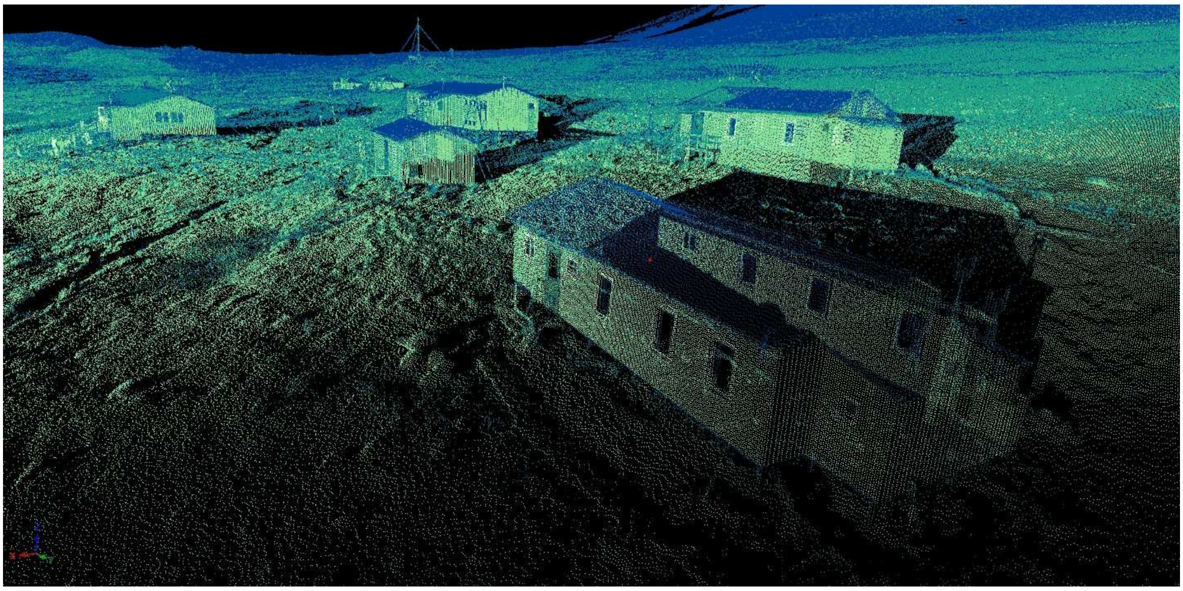

Figure 4. *Screenshot of raw point cloud to demonstrate registration (merging) of multiple point clouds. Multiple point clouds generated byt scanning from multiple positions to avoid 'shadows' cast by hills, river banks, boulders and buildings, for example.*

High-resolution topography of the upper Tarfala valley

Jonathan L. Carrivick, Mark W. Smith, Daniel M. Carrivick

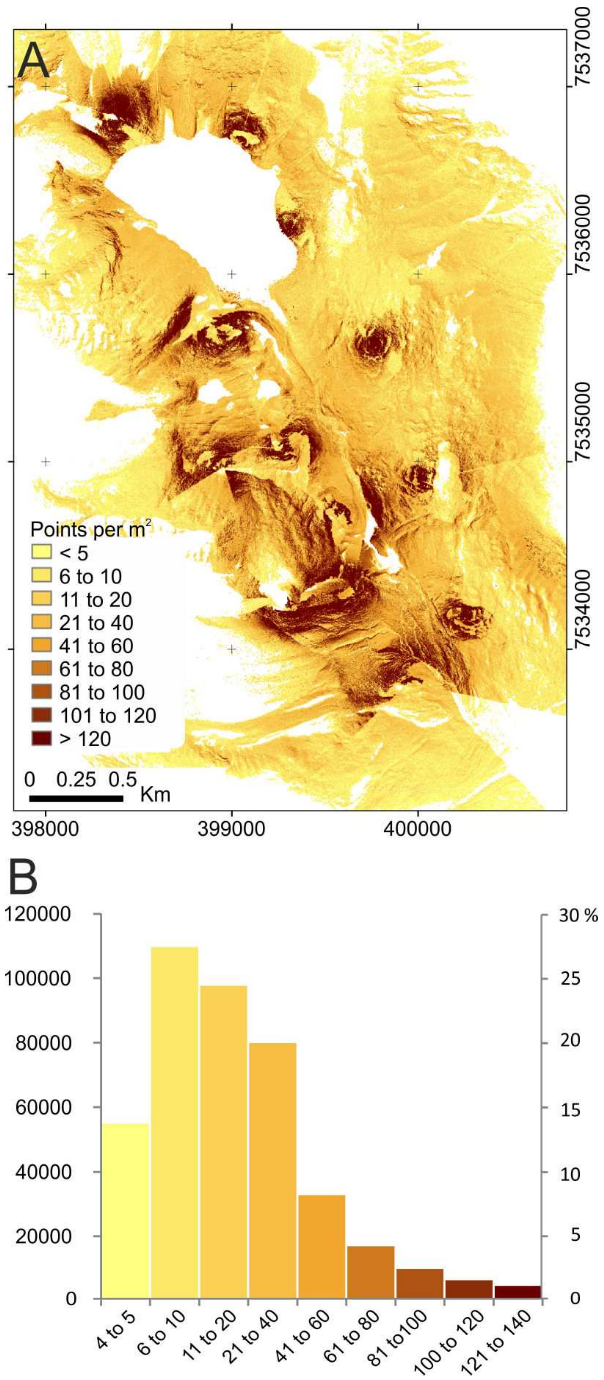

Figure 5. *Number of laser scanner returns, or '3D points' per square metre, represented spatially (A) and in frequency (B). Note that this spatial density was obtained by setting a 0.2 m point spacing at 200 m range. For interpreting the accuracy of our gridded elevation model, which takes the mean of points within a 1 m grid cell, (B) highlights that 85% of 1 m² grid cells have > 10 associated elevation points.*

High-resolution topography of the upper Tarfala valley

Jonathan L. Carrivick, Mark W. Smith, Daniel M. Carrivick

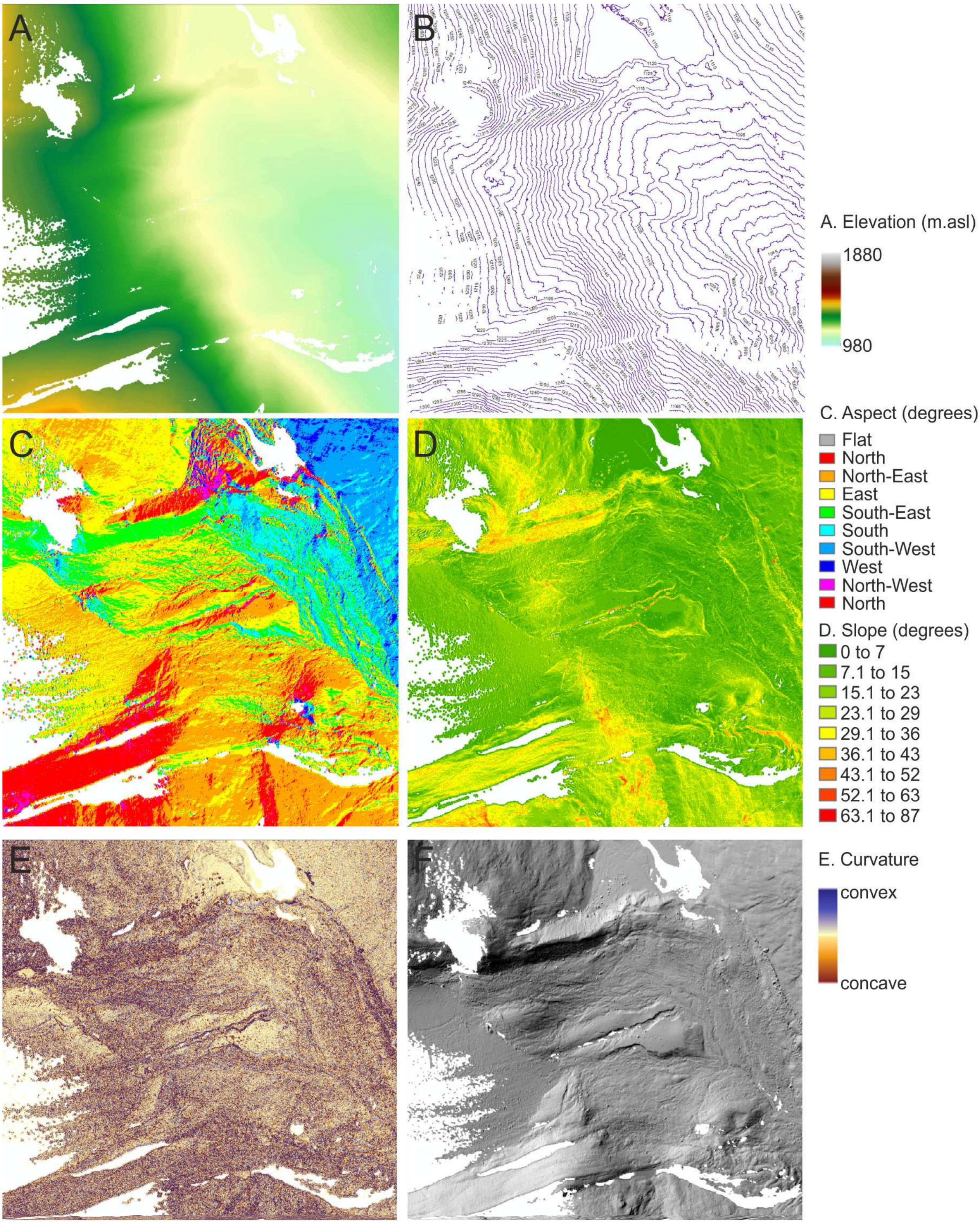

Figure 6. *First and second order derivatives of topography for a 1 km^2 area; specifically the Storglaciären proglacial area or 'forefield', namely elevation surface (A), digital contours at 5 m interval (B), slope (C), aspect (D), curvature (E) and hillshaded terrain (F).*

High-resolution topography of the upper Tarfala valley

Jonathan L. Carrivick, Mark W. Smith, Daniel M. Carrivick

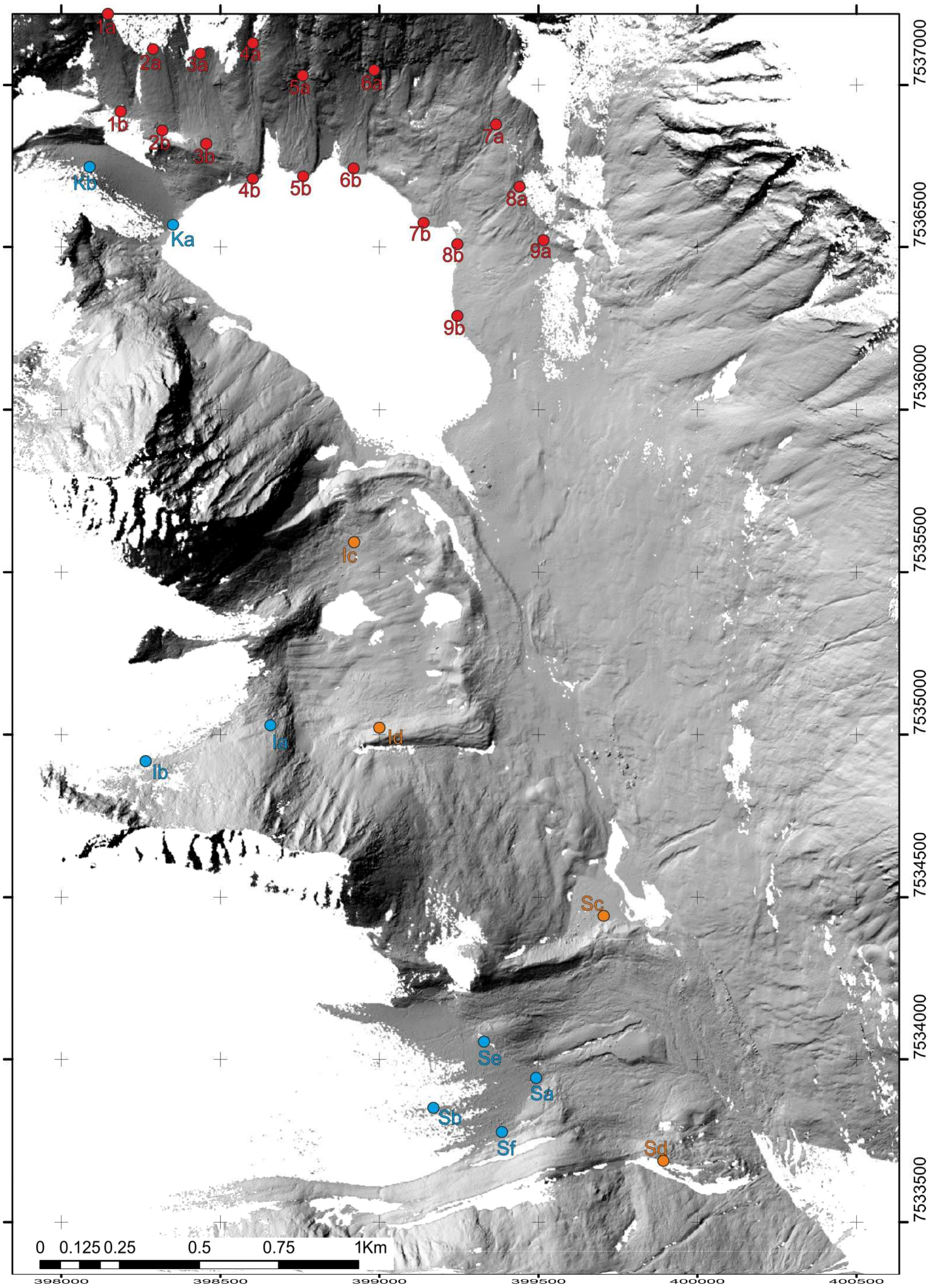

Figure 7. *Overview of topography of Tarfala valley, as represented by a hillshaded 1m grid resolution digital elevation model. Numbered dots refer to ends of transects depicted in Figure 8. Some of the major landforms visible include glacier termini, moraines, talus/scree slopes, debris and alluvial fans, fluvial gravel surfaces. The white areas denote 'missing data' where laser drop-out occurred due to a wet surface (e.g. lake, river), shading (e.g. behind major moraine crest) or being out of range given material property (e.g. glacier surface, lowermost easternmost part of valley floor).*

High-resolution topography of the upper Tarfala valley

Jonathan L. Carrivick, Mark W. Smith, Daniel M. Carrivick

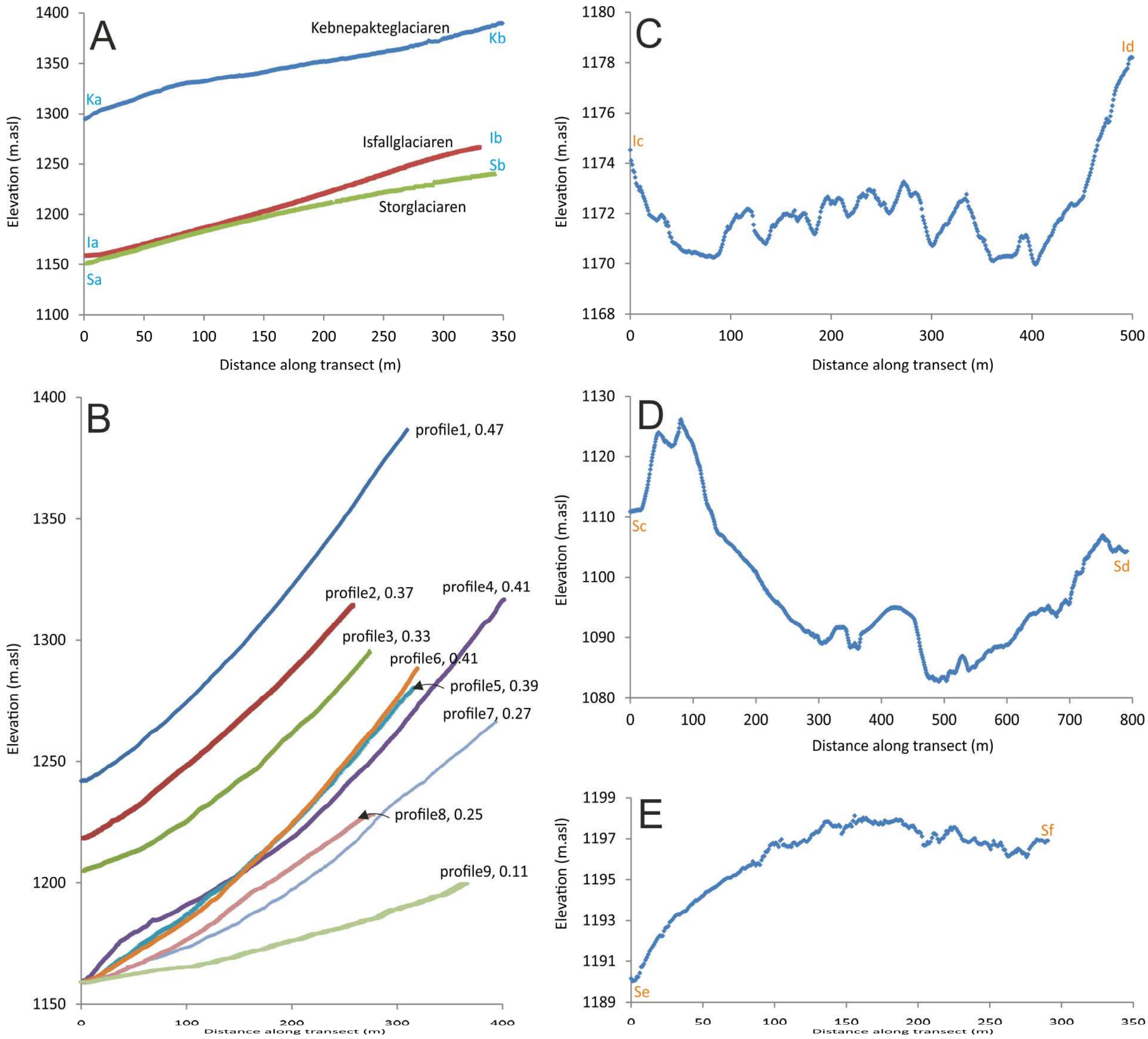

Figure 8. *Transects as marked in Figure 7 of elevation at selected sites of interest: namely flow-parallel transects on lowermost part of glacier ablation area (A), centre-line profiles on mass movement deposits (B), palaeoflow-transverse forefield transects at Isfallsglaciaren (C) and at Storglaciaren (D), and flow-transverse transect on Storglaciaren surface (E). Note varying x and y scales, and vertical exaggeration.*

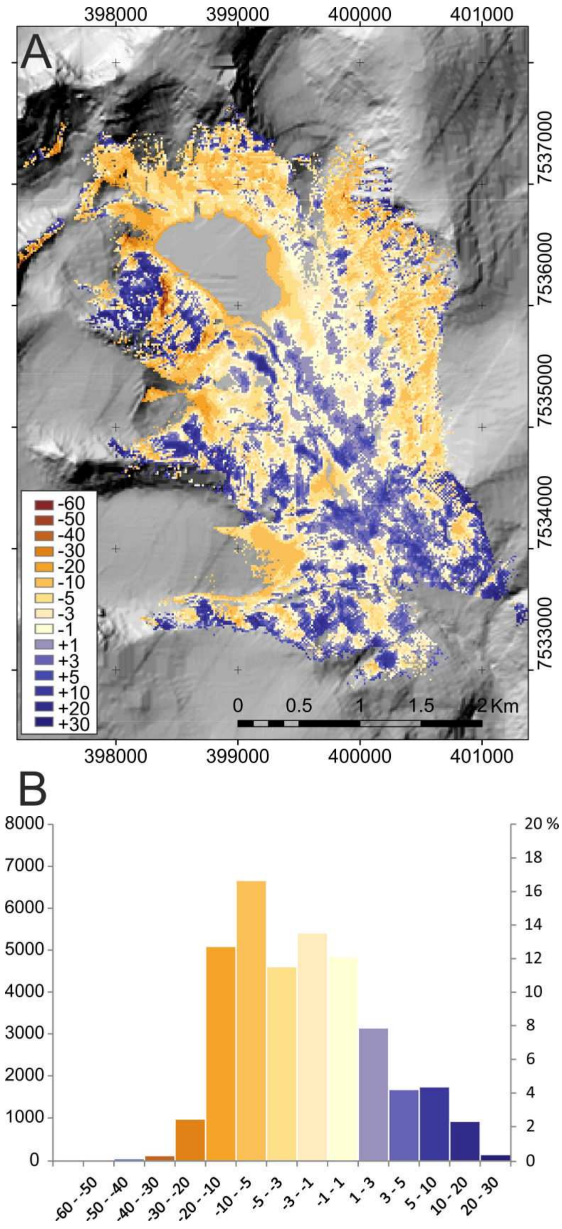

Figure 9. *Difference in elevation (metres) spatially (A) and in frequency (B) between the 1 m grid resolution digital elevation model of this study and the 15 m grid resolution digital elevation model of Johansson et al. (1999), which was produced by digitising the Holmlund and Schytt (1987) hard copy map. Note positive values in this figure mean that the 1m DEM is higher than the 15 m DEM. Background image is the hillshaded 15 m DEM.*

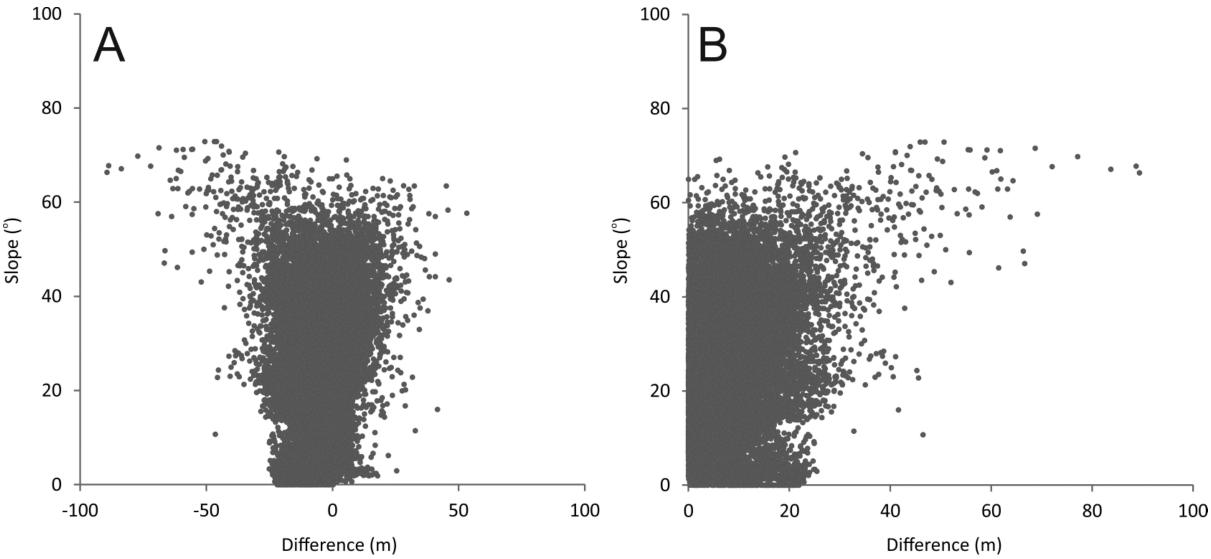

Figure 10. *Raw (A) and absolute (B) difference in elevation (metres) between the 1 m grid resolution DEM of this study and the 15 m grid resolution digital elevation model of Johansson et al. (1999), which was produced by digitising the Holmlund and Schytt (1987) hard copy map. Note positive raw values in panel (A) mean that the 1m DEM is higher than the 15 m DEM.*

High-resolution topography of the upper Tarfala valley

Jonathan L. Carrivick, Mark W. Smith, Daniel M. Carrivick

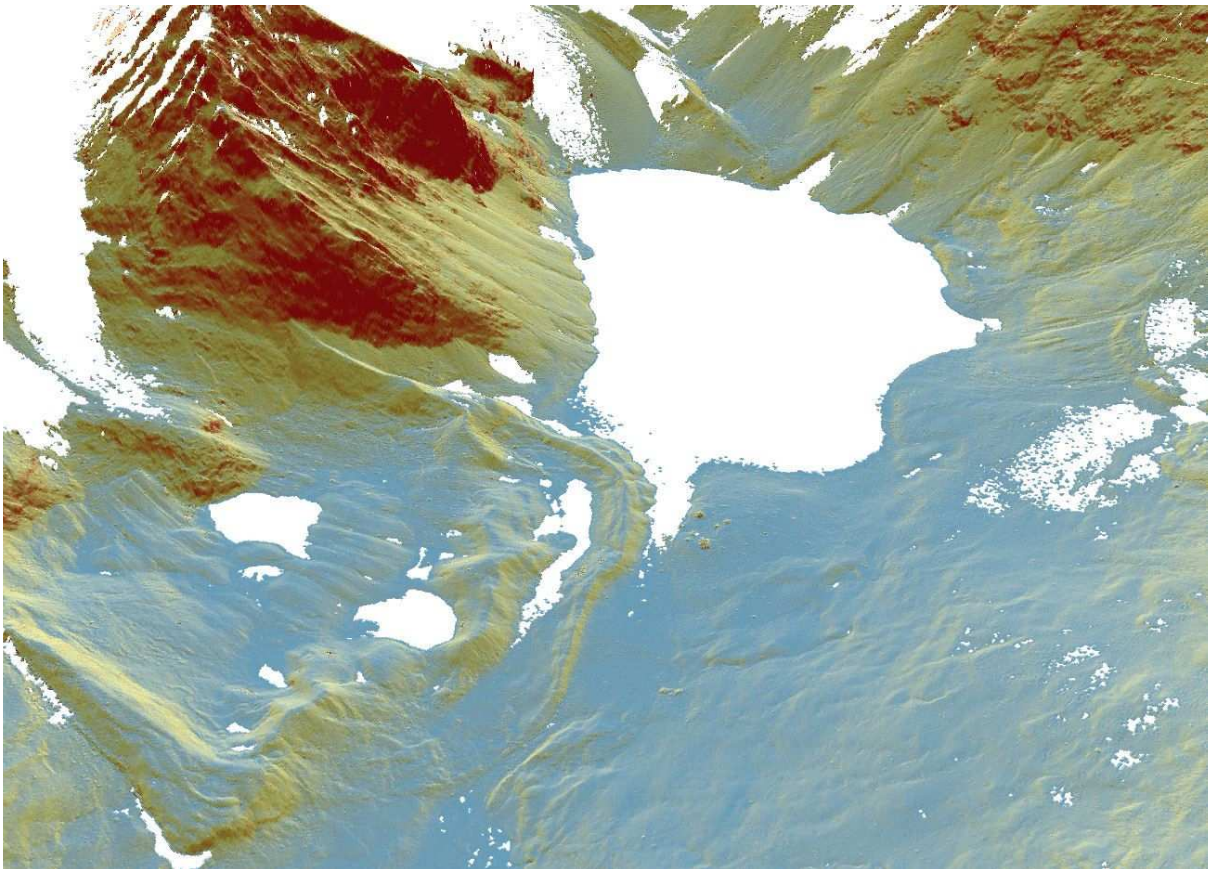

Figure 11. *3D visualisation towards north-west of upper Tarfala valley with slope layer at 50% transparency overlaid on hillshaded terrain layer, both layers projected with base heights from 1 m DEM. Some of the major landforms visible include glacier termini, moraines, talus/scree slopes, debris and alluvial fans, fluvial gravel surfaces. The white areas are 'no data' primarily due to being surface water (lake, river).*